Accepted on Feb. 10 2019 for the publication in
Challenge Journal of Structural Mechanics 5 (1) 2019 9-18

Dynamic instability of castellated beams subjected to transverse periodic loading

Sahar Elaiwi[1], Boksun Kim[2], Long-yuan Li[3]

[1]PhD Student in Structural Engineering, University of Plymouth
(email: sahar.elaiwi@plymouth.ac.uk)

[2]Lecturer in Structural Engineering, University of Plymouth
(email: boksun.kim@plymouth.ac.uk)

[3]Professor of Structural Engineering, University of Plymouth
(email: long-yuan.Li@plymouth.ac.uk)

Abstract – In this study, an analytical solution is developed for the investigation of free vibration, static buckling and dynamic instability of castellated beams subjected to transverse periodic loading. Bolotin's method is used to perform the dynamic instability analysis. By assuming the instability modes, the mass, stiffness, and geometric stiffness matrices are derived using the kinetic energy, strain energy and potential of applied loads. Analytical equations for determining the free vibration frequency, critical buckling moment, and excitation frequency of castellated beams are derived. In addition, the influences of the flange width of the castellated beam and the static part of the applied load on the variation of dynamic instability zones are discussed.

Keywords: castellated beam, buckling, dynamic instability, vibration frequency, lateral-torsional.

1. Introduction

Technological developments in all areas of construction are encouraging researchers and engineers as well as designers in the field to improve the performance of structural members of construction. The castellated beam is one of the steel members, which uses less material but has equal performance as the I-beam of the same size. The fabrication process of castellated beams leads to an increase of beam's depth and thus the bending strength and stiffness about the major axis without adding additional materials. This leads to use castellated beams in the long span applications subject to light or moderate loading conditions for supporting floors and roofs. However, the castellated beams have web openings, which may reduce the shear resistance of the beam. Additionally, the presence of web openings also causes a decrease of the overall sectional torsional stiffness, which may decrease the resistance of the beam to lateral-torsional buckling. Kerdal (1982) and Demirdjian (1999) reported that the torsional stiffness of the web is affected by the depth and slenderness of the beam. A number of experimental, theoretical and numerical investigations have showed the factors having an impact on castellated beam's vulnerability to lateral torsion buckling, which include the distance between the lateral restrictions to the compression stresses of the flanges; properties of the material; boundary conditions; type of cross section; type and position of the loading; quantity and distribution of the residual stresses and geometric imperfections. Previous studies investigated the lateral-torsional buckling (Kerdal and Nethercot ,1982; Mohebkhah,2004; Korrani et al., 2010; Sonck et al., 2014; Kim et al., 2016 ; Kwani and Wijaya,2017) and lateral buckling (Müller et al., 2006 ; Showkati et al.,2012) of castellated beams under transverse loads.

Literature survey on structural members shows that little research has been carried out on the dynamic instability of castellated beams when the applying load varies with time. In many countries, the static load still dominates the current designing of structures for castellated beams, in spite of the significance of the dynamic response to machinery loading and to extreme environmental loads; for example, wind and earthquakes, that have been considered for some time. It is acknowledged that applying dynamic load can lead to the vibration

of structural members, which causes a decrease in the critical load of buckling of the members. For this reason, we should understand the effect of applying the dynamic load on the structural behaviour to avoid resonance disasters due to the dynamic instability.

Limited research and studies exist on the dynamics, especially the dynamic instability of castellated beams subjected to transverse loading. Since 1960 research has been carried out on the vibration-induced buckling of beams. For instance, Morris (1965) investigated the nonlinear vibration problem of a two hinged beam-column subjected to a harmonic load of any space distribution. Hsu (1966) carried out the investigation of the dynamic stability of the elastic body with given initial conditions and reported the necessary and sufficient stability criteria in terms of trajectories in the phase space of finite dimension. Huang (1980) and Chen et al. (1991) used the Bolotin's method to examine the dynamic instability of generally orthotropic beams and thick bi-modulus beams subjected to periodic axial loads, respectively. The Routh-Hurwitz stability and the averaging method have been used by Huang and Hung (1984) to study the dynamic instability of a simply supported beam subjected to periodic axial excitation. The coupling of the first two modes was considered to investigate the instability regions and vibration amplitudes. Many researchers discussed the influences of both the natural frequencies and static buckling loads on the dynamic instability behaviour. Gürgöze (1985) conducted an investigation into the instability behaviour of a pre-twisted beam subjected to a pulsating axial load. He used the Mettler method and derived the equations describing the instability regions that could be applied with different boundary conditions. A finite element dynamic instability model of Timoshenko beams was introduced by Park (1987), which adopted the extended Hamilton's principle to build the equation of the beam transverse motion in the plane. Another study was carried out by Kar and Sujata (1991), who examined the dynamic instability of rotating beams with various different boundary conditions subjected to a pulsating axial excitation. They also discussed the influences of the boundary conditions and rotational speed on the static buckling loads and the zones of parametric instability. Yeh et al. (2004) used the harmonic balance method and the finite element method to investigate the dynamic instability problem of a sandwich beam with a constrained layer and an electro rheological fluid core subjected to an axial dynamic force. Zhu et al. (2017) presented an analytical solution to examine the free vibration, static buckling and dynamic instability of laterally-restrained zed-section purlin beams under uplift wind loading. They used the classical principle of minimum potential energy, in which the kinetic energy and strain energy of the beam and the loss of the potential energy of the applied load are evaluated by assuming instability modes. The influence of different supporting boundary conditions on the dynamic instability behaviour of beams has been also studied by Uang and Fan (2001); Yoon and Kim (2002). More recently, Zhu et al. (2018) presented a study on the dynamic buckling of cold-formed steel channel section beams under the action of uniformly distributed loading. Gao et al. (2019) provided a nondeterministic dynamic stability assessment of Euler–Bernoulli beams using Chebyshev surrogate model.

In this study, an analytical solution is developed to investigate the free vibration, static buckling and dynamic instability of castellated beams subjected to transverse periodic loading. Bolotin's method is used to perform the dynamic instability analysis. By assuming the instability modes, the mass, stiffness, and geometric stiffness matrices are derived using the kinetic energy, strain energy and potential of applied loads. Analytical equations for determining the free vibration frequency, critical buckling moment, and excitation frequency of castellated beams are derived. In addition, the influences of the flange width of the castellated beam and the static part of the applied load on the variation of dynamic instability zones are discussed

2. Governing equations for dynamic instability analysis of castellated beams

The analysis model used for this study is illustrated in Fig. 1(a). The cross-section of the castellated beam is assumed to be doubly symmetric, with the flange width and thickness as $\boldsymbol{b_f}$ and $\boldsymbol{t_f}$, the web depth and thickness as h_w and t_w, and the half depth of hexagons as a. The half of the distance between the centroids of the two T-sections is e. The side length of the hexagonal opening is $\left(\frac{2a}{\sqrt{3}}\right)$, and the hexagonal opening height is $2a$, respectively.

According to Fig. 1 (b), the lateral and transverse displacements of the beam are assumed to be v(x) and w(x), respectively, and the angle of twist of the cross-section is $\phi(x)$. The strain energy of the beam involves two parts; the strain energy generated by the bending and the strain energy generated by the twist.

In order to consider the warping influence, the cross-section of the castellated beam is decomposed into three parts, two of which represent the top and bottom T-sections, one of which represents the middle-part of the web. It is assumed that the displacements at the shear canters of the top and bottom tee-sections are small and can be expressed as follows (see **Fig. 1**) (Kim et al., 2016):

$$v_1(x) = v(x) + \frac{h}{2}\phi(x) \tag{1}$$

$$v_2(x) = v(x) - \frac{h}{2}\phi(x) \tag{2}$$

$$w_1(x) = w + \frac{h}{2}(1 - cos\phi) \approx w \tag{3}$$

$$w_2(x) = w + \frac{h}{2}(1 - cos\phi) \approx w \tag{4}$$

where v_1 and v_2 are the lateral displacements of the shear centers of the top and bottom T-sections, w_1 and w_2 are the transverse displacements of the shear centers of the top and bottom T-sections, *h* is the distance between the shear centers of top and bottom T-sections. The kinetic energy, *T*, of the castellated beam due to the lateral and transverse displacements, and the rotation of the section thus can be expressed as:

The kinetic energy for the top T- section:

$$T_{top} = \frac{\rho A_{tee}}{2}\int_0^l (\dot{v_1}^2 + \dot{w_1}^2)dx + \frac{\rho I_{ptop}}{2}\int_0^l \dot{\phi}^2\, dx \tag{5}$$

The kinetic energy for the bottom T- section:

$$T_{bot} = \frac{\rho A_{tee}}{2}\int_0^l (\dot{v_2}^2 + \dot{w_2}^2)dx + \frac{\rho I_{pbot}}{2}\int_0^l \dot{\phi}^2\, dx \tag{6}$$

The kinetic energy for the middle part between the two T- sections

$$T_{web} = \frac{\rho 2at_w}{2}\int_0^l (\dot{v}^2 + \dot{w}^2)dx + \frac{\rho I_{pweb}}{2}\int_0^l \dot{\phi}^2\, dx \tag{7}$$

Hence, the total kinetic energy of the beam is:

$$T = \frac{\rho}{2}\left[A_{tee}\left[\int_0^l (\dot{v_1}^2 + \dot{w_1}^2)dx + \int_0^l (\dot{v_2}^2 + \dot{w_2}^2)dx\right] + at_w\int_0^l (\dot{v}^2 + \dot{w}^2)dx + I_p\int_0^l \dot{\phi}^2\, dx\right] \tag{8}$$

Where ρ is the density, l is the beam length, $A_{tee=}b_f t_f + t_w\left(\frac{h_w}{2} - a\right)$ is the cross-section area of the T-section, $I_p = I_{pbot} + I_{pweb} + I_{ptop}$ is the polar moment of inertia. Note that the dot above a symbol in above equations represents the derivative of the symbol with respect to time.

The strain energy of the castellated beam is also determined based on the three parts due to the transverse displacement, lateral displacement and rotation. It thus can be written as follows:

$$U_s = \frac{1}{2}\int_0^l \left[EI_{y1}\left(\frac{d^2w_1}{dx^2}\right)^2 + EI_{z1}\left(\frac{d^2v_1}{dx^2}\right)^2 + GJ_1\left(\frac{d\phi}{dx^2}\right)^2 \right] dx + \frac{1}{2}\int_0^l \left[EI_{y2}\left(\frac{d^2w_2}{dx^2}\right)^2 + EI_{z2}\left(\frac{d^2v_2}{dx^2}\right)^2 + GJ_2\left(\frac{d\phi}{dx^2}\right)^2 \right] dx + \frac{1}{2}\int_0^l \left[EI_{y3}\left(\frac{d^2w_3}{dx^2}\right)^2 + EI_{z3}\left(\frac{d^2v_3}{dx^2}\right)^2 + GJ_3\left(\frac{d\phi}{dx^2}\right)^2 \right] dx \quad (9)$$

where U_s is the strain energy, *E* is the Young's modulus, *G* is the shear modulus. $I_{y1} = I_{y2}$ and $I_{z1} = I_{z2}$ are the second moments of the T- sectional area about the *y* and *z* axes. $J_1 = J_2$ is the torsional constant of the T-section, I_{y3} and I_{z3} are the second moments of the cross-sectional area of the mid-part of the web about the *y* and *z* axes, respectively, and J_3 is the torsional constant of the mid-part of the web.

Hence, the formula of the strain energy of castellated beam (top T- sections, bottom T- sections and mid-part of the web) can be written as follows:

$$U = \frac{1}{2}\int_0^l \left[2EI_{y1}\left(\frac{d^2w_1}{dx^2}\right)^2 + 2EI_{z1}\left(\frac{d^2v_1}{dx^2}\right)^2 + \frac{h^2}{2}EI_{z1}\left(\frac{d^2\phi}{dx^2}\right)^2 + 2GJ_1\left(\frac{d\phi}{dx^2}\right)^2 \right] dx + \frac{1}{2}\int_0^l \left[EI_{y3}\left(\frac{d^2w_2}{dx^2}\right)^2 + EI_{z3}\left(\frac{d^2v_2}{dx^2}\right)^2 + GJ_3\left(\frac{d\phi}{dx^2}\right)^2 \right] dx \quad (10)$$

According to **Fig. 1,** I_{y1} , I_{z1} and J_1 are constants, whereas I_{y3} , I_{z3} and J_3 are the function of *x* and dependent upon the location of the web openings. Note, from the comparison between equation of the strain energy of an I-beam without web openings and Eq (10), the following relations can be obtained:

$$I_y = 2I_{y1} + I_{y3} \quad (11)$$

$$I_z = 2I_{z1} + I_{z3} \quad (12)$$

$$I_w = \left(\frac{h}{2}\right)^2 I_z \approx \frac{h^2}{2} I_{z1} \quad (13)$$

$$J = 2J_1 + J_3 \quad (14)$$

$$I_p = I_y + I_z = 2I_{y1} + 2I_{z1} + kI_{y3} + kI_{z3} \quad (15)$$

According to the work (Kim et al., 2016), k refers to the fraction of the volume of the solid and holes in the mid-part of the web . In castellated beams, because of matching of the solid areas and holes in the mid-part of the web, the value of *k*=0.5 is taken.

Assume that the transverse load is the periodic load applying on the top flange of castellated beam when the sheeting is fixed with the top flange (e.g. for wind-induced vibration). In this case, the loss of potential energy V of the transverse load q_z can be expressed as follows:

$$V = \int_0^l \left[M_y\phi\left(\frac{d^2v}{dx^2}\right) + \frac{a_z q_z}{2}\phi^2 \right] dx \quad (16)$$

where q_z is the distribution load, M_y is the pre-buckling internal bending moment, and a_z refers to the *z*-coordinate of the loading point, which is equal to the distance between the loading point and the shear centre of the beam. In the present case, $a_z = \frac{h_w}{2} + t_f$ because the uniformly distributed load is applied on the top

flange of the beam. The second term in Eq. (16) is attributed to the effect of loading position, which, in the present case, has a positive effect on the stability of the beam and thus will increase the critical buckling load.

According to the Lagrange method, the equations of motion describing the lateral-torsional buckling of the beam can be expressed as follows:

$$\frac{d}{dt}\left(\frac{\partial L}{\partial \dot{q}}\right) - \frac{\partial L}{\partial q} = 0 \tag{17}$$

where $L = T - (U - V)$ is the Lagrangian function, and q is the general displacement vector. Substituting Eqs (1)-(4), (8), (10), (16) into (17), the governing equation for the dynamic instability analysis of a castellated beam is obtained as follows (Kratzig and Nawrotzki, 1991; Li, 1991; Patel et al, 2006)

$$[\mathbf{M}]\{\ddot{\mathbf{q}}\} + [\mathbf{K}]\{\mathbf{q}\} - \lambda\left[\mathbf{K_g}\right]\{\mathbf{q}\} = \{0\} \tag{18}$$

where **[M]** is the mass matrix, **[K]** is the elastic stiffness matrix, $\mathbf{[K_g]}$ is the geometric stiffness matrix, $\{\ddot{\mathbf{q}}\}$ is the generalized acceleration vector, $\{\mathbf{q}\}$ is the general displacement vector, and λ is the loading factor. The mass, stiffness, and geometric stiffness matrices are expressed as follows:

$$[\mathbf{M}] = \begin{bmatrix} \frac{\partial^2 T}{\partial \dot{q}_1^2} & \frac{\partial^2 T}{\partial \dot{q}_1 \partial \dot{q}_2} & \frac{\partial^2 T}{\partial \dot{q}_1 \partial \dot{q}_3} \\ \frac{\partial^2 T}{\partial \dot{q}_2 \partial \dot{q}_1} & \frac{\partial^2 T}{\partial \dot{q}_2^2} & \frac{\partial^2 T}{\partial \dot{q}_2 \partial \dot{q}_3} \\ \frac{\partial^2 T}{\partial \dot{q}_3 \partial \dot{q}_1} & \frac{\partial^2 T}{\partial \dot{q}_3 \partial \dot{q}_2} & \frac{\partial^2 T}{\partial \dot{q}_3^2} \end{bmatrix} \tag{19}$$

$$[\mathbf{K}] = \begin{bmatrix} \frac{\partial^2 U}{\partial q_1^2} & \frac{\partial^2 U}{\partial q_1\, \partial q_2} & \frac{\partial^2 U}{\partial q_1\, \partial q_3} \\ \frac{\partial^2 U}{\partial q_2\, \partial q_1} & \frac{\partial^2 U}{\partial q_2^2} & \frac{\partial^2 U}{\partial q_2\, \partial q_3} \\ \frac{\partial^2 U}{\partial q_3\, \partial q_1} & \frac{\partial^2 U}{\partial q_3\, \partial q_2} & \frac{\partial^2 U}{\partial q_3^2} \end{bmatrix} \tag{20}$$

$$\left[\mathbf{K}_g\right] = \begin{bmatrix} \frac{\partial^2 V}{\partial q_1^2} & \frac{\partial^2 V}{\partial q_1\, \partial q_2} & \frac{\partial^2 V}{\partial q_1\, \partial q_3} \\ \frac{\partial^2 V}{\partial q_2\, \partial q_1} & \frac{\partial^2 V}{\partial q_2^2} & \frac{\partial^2 V}{\partial q_2\, \partial q_3} \\ \frac{\partial^2 V}{\partial q_3\, \partial q_1} & \frac{\partial^2 V}{\partial q_3\, \partial q_2} & \frac{\partial^2 V}{\partial q_3^2} \end{bmatrix} \tag{21}$$

Assume that the externally applied load q_z is periodic loading, in which case the loading factor can be divided into two parts as expressed as follows:

$$\lambda = \lambda_s + \lambda_t \cos\Omega t \tag{22}$$

where λ_s and λ_t are the amplitudes of the static and dynamic parts, respectively, Ω is the excitation frequency of the dynamic part of the load, and t is the time.

The dynamic instability regions of the beam described by Eq. (18) can be calculated by investigating periodic solutions with the periods of T=2π/Ω and 2T=4π/Ω. The solution with the period of 2T is of particular

importance, representing the primary instability region of the structure, which can be expressed using the form of trigonometric series given by:

$$\{\boldsymbol{q}\} = \sum_{k=1,3,\ldots} \left[\{\boldsymbol{a_k}\} sin\frac{k\Omega t}{2} + \{\boldsymbol{b_k}\} cos\frac{k\Omega t}{2}\right] \tag{23}$$

where $\{\boldsymbol{a_k}\}$ and $\{\boldsymbol{b_k}\}$ are the vectors of coefficients of the assumed solution. Substituting Eqs. (22) and (23) into (18) and letting the coefficients of the series associated with sin (Ωt/2) and cos (Ωt/2) be zero, it yields:

$$\left([\mathbf{K}] - \frac{2\lambda_s - \lambda_t}{2}[\mathbf{K}_g] - \frac{\Omega^2}{4}[\mathbf{M}]\right)\{\boldsymbol{a_1}\} = \{\mathbf{0}\} \tag{24}$$

For given values of λ_s and λ_t one can calculate the two frequencies of Ω from Eqs. (24) and (25), which

$$\left([\mathbf{K}] - \frac{2\lambda_s + \lambda_t}{2}[\mathbf{K}_g] - \frac{\Omega^2}{4}[\mathbf{M}]\right)\{\boldsymbol{b_1}\} = \{\mathbf{0}\} \tag{25}$$

represent the boundary of dynamic instability region of the castellated beams under periodic loading.

3. Simply supported, doubly symmetric castellated beam subjected to periodic loads on top flange

For the calculation due to the dynamic lateral-torsional buckling, the displacement functions *w(x)*, *v(x)*, *ϕ(x)* and pre-buckling internal bending moment $M_y(x)$ that satisfy the boundary conditions of a simply supported beam can be assumed as follows:

$$v(x) = q_1(t) sin\frac{\pi x}{l} \tag{26}$$

$$w(x) = q_2(t) sin\frac{\pi x}{l} \tag{27}$$

$$\phi(x) = q_3(t) sin\frac{\pi x}{l} \tag{28}$$

$$M_y(x) = \frac{q_z x(l-x)}{2} \tag{29}$$

where $q_i(t)$ $(i = 1,2,3)$ are the functions of time *t*.

Therefore, the mass, stiffness, and geometric stiffness matrices for simply supported beam are obtained from Eqs. (19)- (21) and are expressed as follows:

$$[\mathbf{M}] = \begin{bmatrix} m_{11} & 0 & 0 \\ 0 & m_{22} & 0 \\ 0 & 0 & m_{33} \end{bmatrix} \tag{30}$$

where:

$$m_{11} = m_{22} = \rho l(at_w + A_{tee}) \tag{31}$$

$$m_{33} = \rho l\left(\frac{A_{tee}h^2}{4} + \frac{I_p}{2}\right) \tag{32}$$

$$[\mathbf{K}] = \begin{bmatrix} \kappa_{11} & 0 & 0 \\ 0 & \kappa_{22} & 0 \\ 0 & 0 & \kappa_{33} \end{bmatrix} \tag{33}$$

where:

$$\kappa_{11} = \frac{El(2I_{z1} + kI_{z3})}{2}\left(\frac{\pi}{l}\right)^4 \tag{34}$$

$$\kappa_{22} = \frac{El\left(2I_{y1} + kI_{y3}\right)}{2}\left(\frac{\pi}{l}\right)^4 \tag{35}$$

$$\kappa_{33} = \frac{EI_w l}{2}\left(\frac{\pi}{l}\right)^4 + \frac{Gl(2J_1 + kJ_3)}{2}\left(\frac{\pi}{l}\right)^2 \tag{36}$$

$$\left[\mathbf{K}_g\right] = \begin{bmatrix} 0 & 0 & \kappa_{g13} \\ 0 & 0 & 0 \\ \kappa_{g31} & 0 & \kappa_{g33} \end{bmatrix} \tag{37}$$

where:

$$\kappa_{g13} = \kappa_{g31} = -\frac{q_z l}{8}\left(\frac{\boldsymbol{\pi^2}}{\mathbf{3}} + 1\right) \tag{38}$$

$$\kappa_{g33} = -\frac{a_z q_z l}{2} \tag{39}$$

3.1. The free vibration analysis

The free vibration frequency of the lateral-torsional vibration of the castellated beam can be determined using Eq. (33):

$$\|[\mathbf{K}] - \omega^2[\mathbf{M}]\| = 0 \tag{40}$$

where ω is the free vibration frequency. Substituting Eqs. (30) and (33) into (39), the following frequency can be obtained:

$$\omega_1 = \left(\frac{\pi}{l}\right)^2 \sqrt{\frac{E(2I_{z1} + kI_{z3})}{2\rho(at_w + A_{tee})}} \tag{41}$$

$$\omega_2 = \left(\frac{\pi}{l}\right)^2 \sqrt{\frac{E\left(2I_{y1} + kI_{y3}\right)}{2\rho(at_w + A_{tee})}} \tag{42}$$

$$\omega_3 = \left(\frac{\pi}{l}\right)^2 \sqrt{\frac{2\left(EI_w + \frac{Gl^2}{\pi^2}(2J_1 + kJ_3)\right)}{\rho\left(A_{tee}h^2 + 2I_p\right)}} \tag{43}$$

I_{z3}^* can be negligible because in most of castellated beams $I_{z3}^* << 2I_{z1}$, then Eqs. (40)- (42) can be simplified as follows:

$$\omega_1 = \left(\frac{\pi}{l}\right)^2 \sqrt{\frac{E(2I_{z1})}{2\rho(at_w + A_{tee})}} \tag{44}$$

$$\omega_2 = \left(\frac{\pi}{l}\right)^2 \sqrt{\frac{E(2I_{y1})}{2\rho(at_w + A_{tee})}} \tag{45}$$

$$\omega_3 = \left(\frac{\pi}{l}\right)^2 \sqrt{\frac{2\left(EI_w + \frac{Gl^2}{\pi^2}(2J_1 + kJ_3)\right)}{\rho\left(A_{tee}h^2 + 2(I_{z1} + I_{y1})\right)}} \tag{46}$$

The above formulations (43), (44) and (45) give the natural frequencies, which are well known and can be found from many vibration textbooks. These equations represent the translational and rotational vibrations of castellated beams. Moreover, it indicates that the lateral vibration and torsional vibration modes are influenced by the web openings.

3.2. Buckling analysis

The critical load of the lateral-torsional buckling of the castellated beam subjected to a static load can be calculated using Eq. (46):

$$\left\|[\mathbf{K}] - \lambda_{cr}[\mathbf{K}_g]\right\| = 0 \tag{46}$$

where λ_{cr} is the loading factor and $q_{cr} = \lambda_{cr} q_z$ is the critical load for static buckling.
Substituting Eqs. (33) and (37) into (46), the following critical load is obtained:

$$\lambda_{cr} = -\frac{K_{11}K_{g33} \pm \sqrt{{K_{11}}^2{K_{g33}}^2 + 4{K_{g13}}^2 K_{11}K_{33}}}{2{K_{g13}}^2} \tag{47}$$

$$\left(\frac{q_z l^2}{8}\right)_{cr} = \frac{\left(\left(\frac{h_w}{2} + t_f\right) + \sqrt{\left(\frac{h_w}{2} + t_f\right)^2 + \frac{1}{4}\left(I_w + \frac{G(2J_1 + kJ_3)}{E}\left(\frac{l}{\pi}\right)^2\right)\left(\frac{\pi^2}{3} + 1\right)^2 \times \frac{1}{(2I_{z1} + I_{z3})}}\right)}{\left(\frac{1}{3} + \frac{1}{\pi^2}\right)^2} \times \frac{2E(2I_{z1} + I_{z3})}{l^2} \tag{48}$$

$$\left(\frac{q_z l^2}{8}\right)_{cr} = \frac{\left(\left(\frac{h_w}{2} + t_f\right) + \sqrt{\left(\frac{h_w}{2} + t_f\right)^2 + \frac{1}{4}\left(I_w + \frac{G(2J_1 + kJ_3)}{E}\left(\frac{l}{\pi}\right)^2\right)\left(\frac{\pi^2}{3} + 1\right)^2 \times \frac{1}{(2I_{z1})}}\right)}{\left(\frac{1}{3} + \frac{1}{\pi^2}\right)^2} \times \frac{2E(2I_{z1})}{l^2} \tag{49}$$

It can be noticed that Eq. (49) is similar to the formulation of the critical load given in the work (Kim et al., 2016) for simply supported castellated beams when the load is applied at the top flange.

3.3. The dynamic instability

The dynamic instability region of the castellated beam can be calculated using Eq. (50):

$$\left\| [\mathbf{K}] - \frac{2\lambda_s \pm \lambda_t}{2} [\mathbf{K}_g] - \frac{\Omega^2}{4} [\mathbf{M}] \right\| = 0 \tag{50}$$

Substituting Eqs. (30)- (37) into (50), it yields:

$$\frac{\Omega^2}{4} = \frac{(K_{33}^* m_{11} + K_{11} m_{33}) \pm \sqrt{(K_{11} m_{33} - K_{33}^* m_{11})^2 + 4\left(\frac{2\lambda_s \pm \lambda_t}{2}\right)^2 {K_{g13}}^2 m_{33} m_{11}}}{2 m_{33} m_{11}} \tag{51}$$

where

$$K_{33}^* = K_{33} - \frac{2\lambda_s \pm \lambda_t}{2} K_{g33} \tag{51}$$

It can be seen that, there are four different equations given by Eq. (51), which represent four different Ω values, where the value of Ω^2 is associated with vibration modes, which were illustrated in the free vibration analysis shown in Section 3.1.

4. Comparison of the dynamic instability of simply supported beams due to transverse periodic loading

Table 1 gives the dimensions and material properties of four castellated beams of different flange widths (*bf* =100 mm, *bf* =150 mm, *bf* =200 mm, and *bf* =250 mm). The analytical solutions used to determine the natural frequencies are obtained directly from Eqs. (43), (44) and (45); while the critical loads are obtained by Eq (49).

Fig. 2, **Fig. 3** and **Fig. 4** present the variation of the frequencies of lateral vibration, vertical vibration and rotational vibration of the beams of different flange widths versus the beam length. The three figures correspond to the 1st, 2nd and 3rd vibration modes.

From these figures it can be observed that, for each vibration mode, the frequency curves have a similar variation pattern. In addition, the beam length and the flange width influence the frequencies. Increasing the beam length causes a reduction in the frequencies. In contrast, the larger flange width gives the greater frequencies. Furthermore, it can be seen from the figures that the frequency of the lateral vibration is slightly higher than the frequency of the rotational vibration of the beam but a little higher than the frequency of the vertical vibration of the castellated beam.

Fig. 5 plots the critical load curves of the beams of different flange widths subjected to the transverse static load applying on the top flange, where the critical moment has been normalized using the yield moment, $M_y = \frac{2\sigma_y I_{reduced}}{h_w + 2t_f}$, where $I_{reduced} = \frac{b_f(h_w+2t_f)^3}{12} - \frac{(2a)^3 t_w}{12} - \frac{(h_w)^3(b_f - t_w)}{12}$. It can be noticed, as expected, that for each beam the increase of beam length causes the reduction of the critical moment.

Figs. 6-9 show the dynamic instability zones of the castellated beams with four different flange widths, subjected to transverse periodic load applied at the top flange of the beam, in which the geometric stiffness matrix is assessed using the static critical load, that is $q_y = q_{cr}$, where $q_y = 16\frac{\sigma_y I_{reduced}}{l^2(h_w+2t_f)}$. The four figures correspond to four different beam lengths as indicated in Table 1. It can be observed from these figures that, the dynamic instability regions of the four beams all exhibit a **"**v**"** shape despite of having different flange widths. With the increase of beam length, the dynamic instability zone not only moves towards to higher frequency side but its width is also expanded. In contrast, where the beam length is the same, the width of the dynamic instability zone decreases with the increase of the flange width.

5. Conclusions

This study has provided an analytical study on the dynamic instability of castellated beams subjected to transverse periodic loading at top flange. The dynamic instability analysis employed in the present study uses Bolotin's method, while the mass, stiffness, and geometric stiffness matrices are derived using the kinetic energy, strain energy and the potential of applied loads. From the obtained results the following conclusions can be drawn:

- The free vibration, static buckling and dynamic instability analyses of castellated beams subjected to transverse periodic loading at the top flange are influenced by the coupling between the translational and rotational modes.

- Increasing the flange width of beam leads to the increase of both the frequency and critical buckling moment. However, increasing beam length reduces this effect.

- The dynamic instability zone of the castellated beam will move towards to high-frequency side and the corresponding width of the dynamic instability zone decreases when its flanges become wide.

- The effect of lateral torsional buckling on the dynamic instability zone becomes more significant in the short beam than in the long beam; and also in the wide flange beam than in the narrow flange beam.

6. Acknowledgement

The first author is grateful to the Ministry of Higher Education and Scientific Research in Iraq to the financial support of her PhD study at the University of Plymouth.

7. References

Bolotin VV (1964). The Dynamic Stability of Elastic Systems. San Francisco, CA, Holden-day, Inc.

Yeh JY, Chen LW, Wang CC (2004). Dynamic stability of a sandwich beam with a constrained layer and electrorheological fluid core. Composite Structures, 64(1), 47-54.

Chen LY, Lin PD, Chen LW (1991). Dynamic stability of thick bimodulus beams, Computers & Structures, 41(2), 257-263.

Demirdjia S (1999). Stability of castellated beam webs. PhD, McGill University Montreal, Canada.

Gao K, Gao W, Wu BH, Song CM (2019). Nondeterministic dynamic stability assessment of Euler–Bernoulli beams using Chebyshev surrogate model. Applied Mathematical Modelling 66, 1-25.

Gürgöze M (1985). On the dynamic stability of a pre-twisted beam subject to a pulsating axial load. Journal of Sound and Vibration, 102(3), 415-422.

Hsu CS (1966). On dynamic stability of elastic bodies with prescribed initial conditions. International Journal of Engineering Science, 4(1), 1-21.

Huang CC (1980). Dynamic stability of generally orthotropic beams. Fibre Science and Technology, 13(3), 187-198.

Huang JS, Hung LH (1984). Dynamic stability for a simply supported beam under periodic axial excitation. International Journal of Nonlinear Mechanics, 19(4), 287-301.

Kar RC, Sujata T (1991). Dynamic stability of a rotating beam with various boundary conditions. Computers & Structures, 40(3), 753-773.

Kazemi Nia Korrani HR, Kabir MZ, Molanaei S (2010). Lateral Torsional Buckling of Castellated Beams Under End Moments. Amirkabir University of Technology.

Kerdal D (1982). Lateral-torsional buckling strength of castellated beams. PhD thesis, Civil and Structural Engineering, Faculty of Engineering (Sheffield), University of Sheffield, Sheffield, UK.

Kim B, Li LY, Edmonds A (2016). Analytical solutions of lateral-torsional buckling of castellated beams. International Journal of Structural Stability and Dynamics, 16(8), 1-16 (1550044).

Kratzig WB, Li LY, Nawrotzki P (1991). Stability conditions for non-conservative dynamical systems. Computational Mechanics, 8(3), 145-151.

Kwani S, Wijaya PK (2017). Lateral torsional buckling of castellated beams analyzed using the collapse analysis. Procedia Engineering, 171, 813–820.

Lagerqvist O, Hedman-Pétursson E, Unosson E, Feldmann M (2006). Large web openings for service integration in composite floors. Design Guide (en), Technical steel report.

Li LY (1991). Interaction of forced and parametric loading vibrations. Computers and Structures, 40(3), 615-618.

Mohebkhah A (2004). The moment-gradient factor in lateral–torsional buckling on inelastic castellated beams. Journal of Constructional Steel Research, 60(10), 1481-1494.

Morris NF (1965). The dynamic stability of beam-columns with a fixed distance between supports. Journal of the Franklin Institute, 280(2), 163-173.

Müller C, Hechler O, Bureau A, Bitar D, Joyeux D, Cajot L G, Demarco T, Lawson RM, Hicks S, Devine P, Showkati H, Ghazijahani TG, Noori A, Zirakian T (2012). Experiments on elastically braced castellated beams. Journal of Constructional Steel Research, 77, 163-172.

Nethercot D, Kerdal D (1982).Lateral-torsional buckling of castellated beams. The Structural Engineer, 60B (3), 53-61.

Park YP (1987). Dynamic stability of a free Timoshenko beam under a controlled follower force. Journal of Sound and Vibration, 113(3), 407-415

Patel SN, Datta PK, Sheikh AH (2006). Buckling and dynamic instability analysis of stiffened shell panels. Thin-Walled Structures, 44(3), 321-333.

Showkati H, Ghazijahani TG, Noori A, Zirakian T (2012). Experiments on elastically braced castellated beams. Journal of Constructional Steel Research, 77, 163-172

Sonck D, Van Impe R, Belis J (2014). Experimental investigation of residual stresses in steel cellular and castellated members. Construction and Building Materials, 54 , 512-519.

Uang CM, Fan CC (2001). Cyclic stability criteria for steel moment connections with reduced beam section. Journal of Structural Engineering, 127(9), 1021-1027.

Yoon SJ, Kim JH (2002). A concentrated mass on the spring unconstrained beam subjected to a thrust. Journal of Sound and Vibration, 254(4), 621-634.

Zhu J, Qian S, Li LY (2017). Dynamic instability of laterally-restrained zed-purlin beams under uplift loading. International Journal of Mechanical Sciences, 131–132, 408–413.

Zhu J, Qian S, Li LY (2018). Dynamic instability of channel-section beams under periodic loading. Mechanics of Advanced Materials and Structures (in press) (https://doi.org/10.1080/15376494.2018.1501521).

Table 1. Dimensions and material properties of castellated beams of different flange widths*

b_f mm	t_f mm	h_w mm	t_w mm	a mm	E GPa	ρ kg/m^3	σ_y MPa	G GPa	v
100	10	300	8	100	210	7800	275	78	0.3
150	10	300	8	100	210	7800	275	78	0.3
200	10	300	8	100	210	7800	275	78	0.3
250	10	300	8	100	210	7800	275	78	0.3

Note*: Dynamic instability analysis uses four different beam lengths. They are 4.156 m; 6.235 m; 9.006 m and 14.549 m

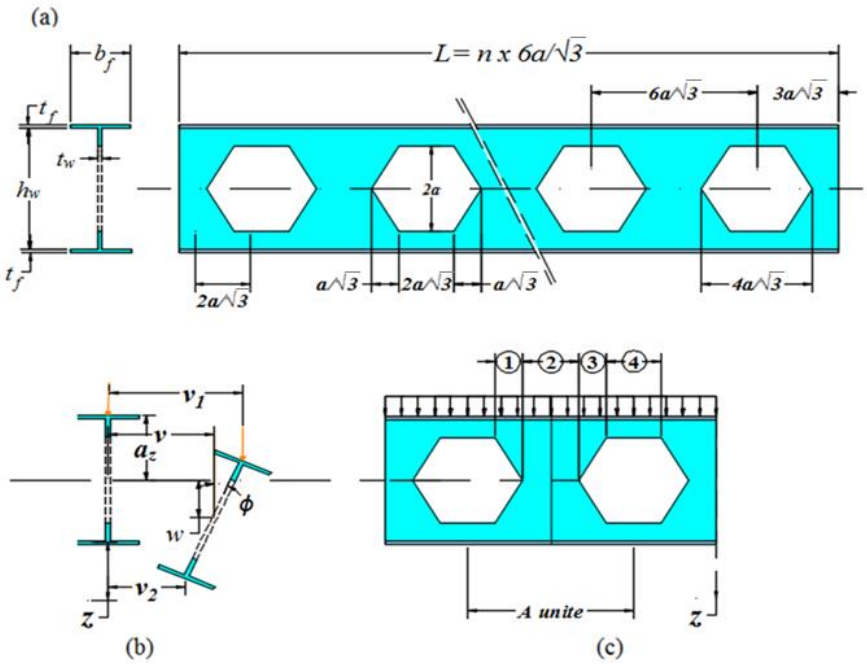

Fig. 1. (a) Notations used in castellated beams. (b) Loading and displacements of web and displacement of flanges when lateral–torsional buckling occurred. (c) Section properties of middle-part of web in four different regions. $I_{y3} = I_{y3}^*$, $I_{z3} = I_{z3}^*$, $J_3 = J_3^*$ in region 2, in region 4,$I_{y3} = I_{z3} = J_3 = 0$, section properties vary with *x* in regions 1 and 3.

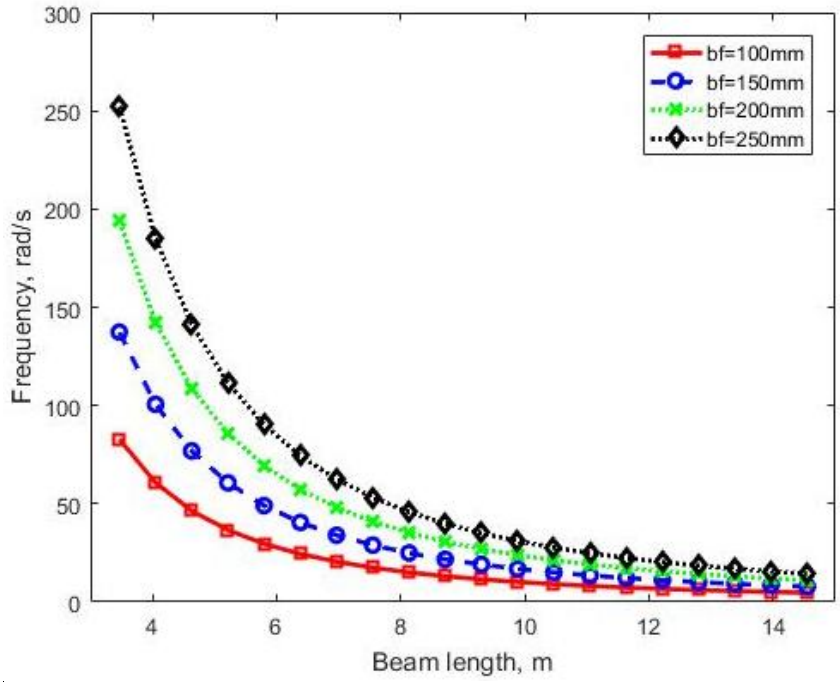

Fig. 2. Comparison of frequencies for simply supported castellated beams with different flange widths (1st mode)

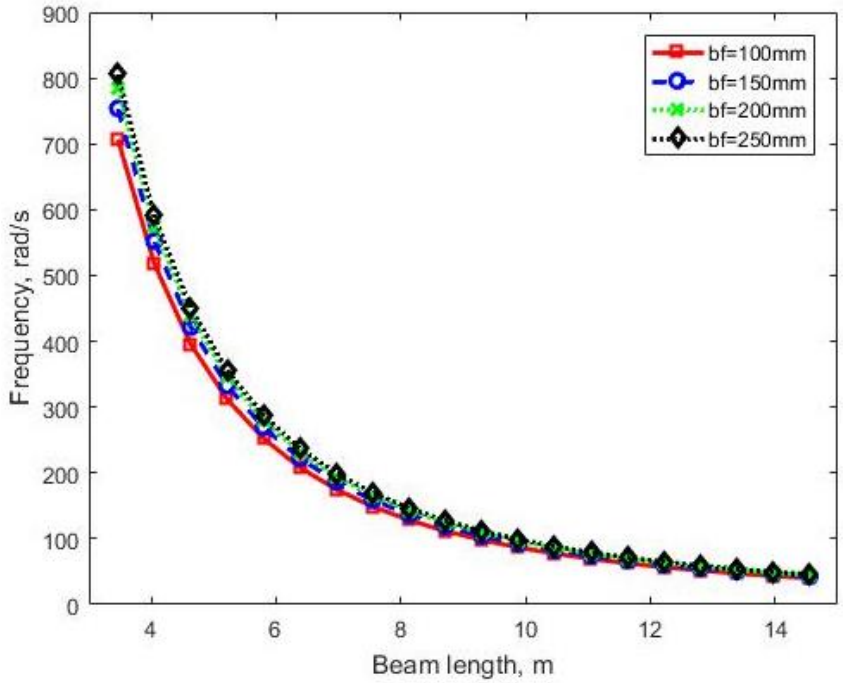

Fig. 3. Comparison of frequencies for simply supported castellated beams with different flange widths (2nd mode)

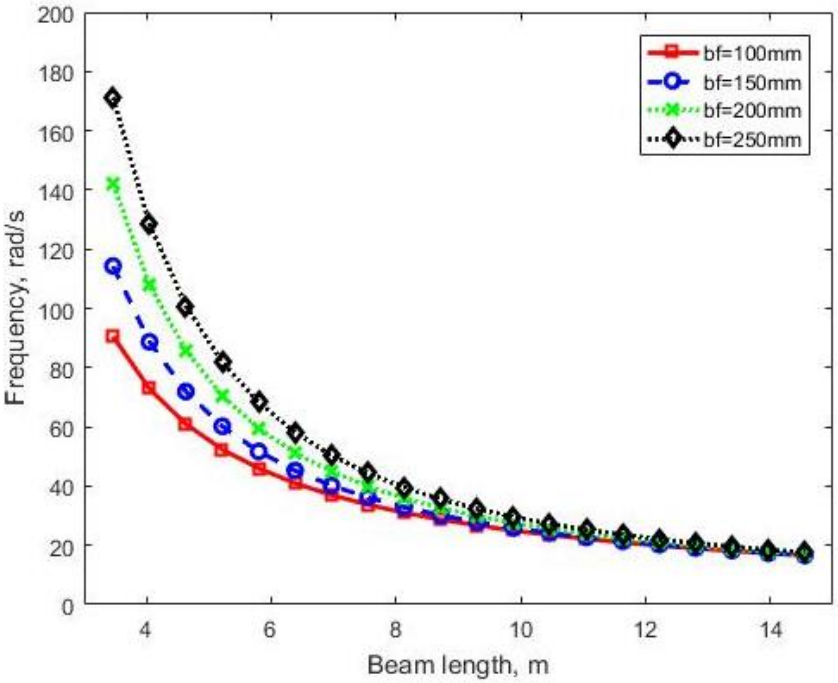

Fig. 4. Comparison of frequencies for simply supported castellated beams with different flange widths (3rd mode)

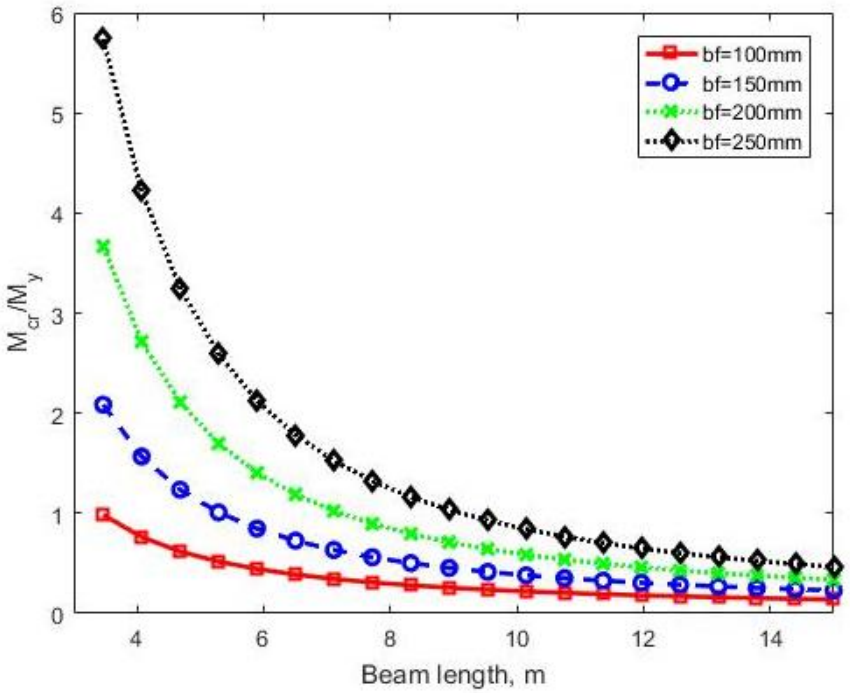

Fig. 5. Comparison of critical buckling moments of simply supported castellated beams with different flange widths

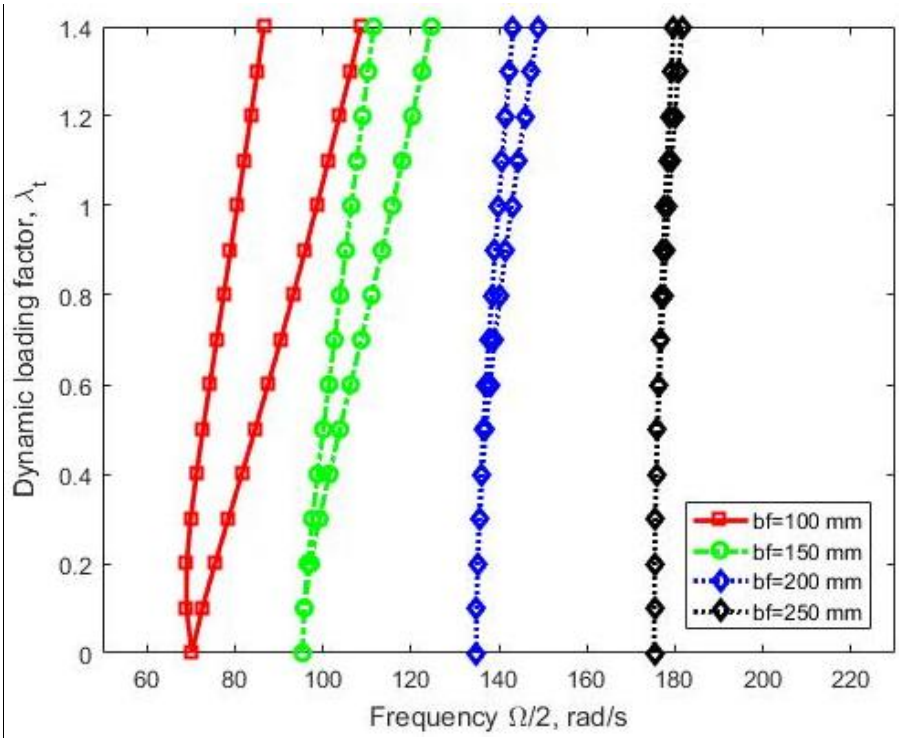

Fig. 6. Comparison of dynamic instability regions of simply supported castellated beams (beam length 4.156 meter) ($q_y = q_{cr}$ **and** λ_s=0)

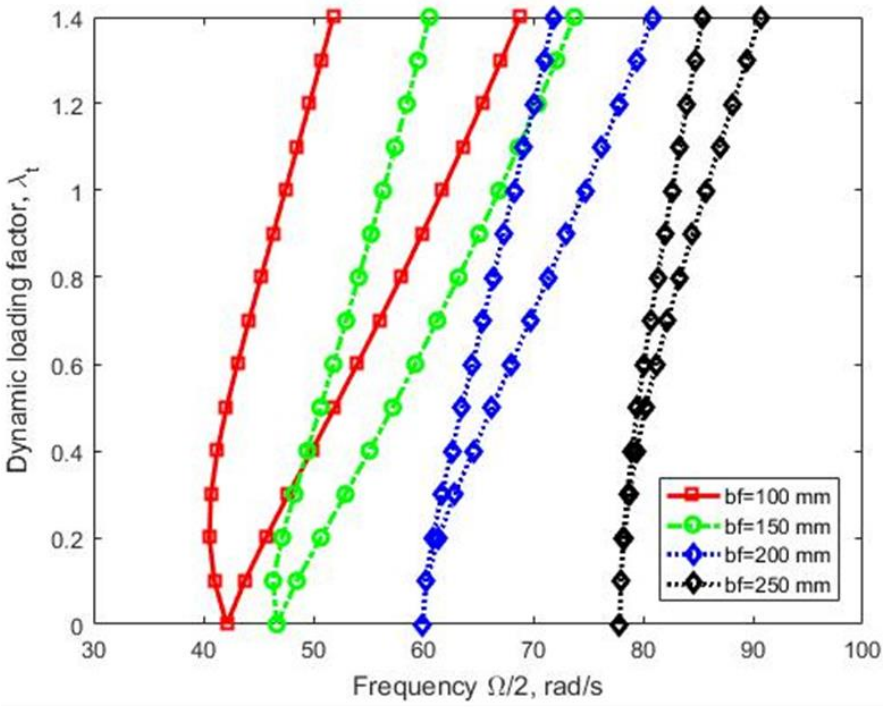

Fig. 7. Comparison of dynamic instability regions of simply supported castellated beams (beam length 6.235 meter) ($q_y = q_{cr}$ **and** λ_s=0)

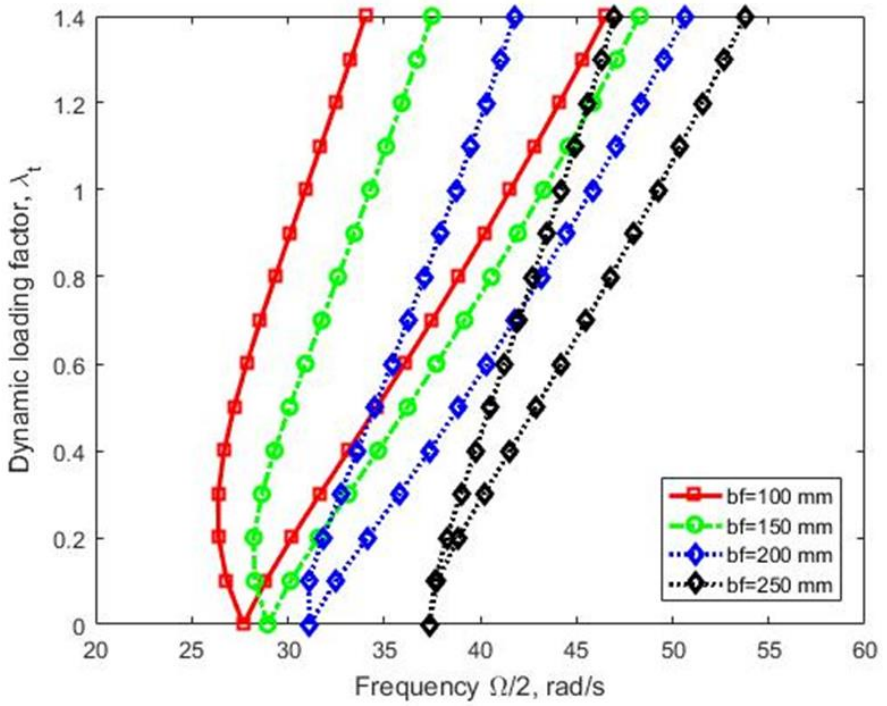

Fig. 8. Comparison of dynamic instability regions of simply supported castellated beams (beam length 9.006 meter) ($q_y = q_{cr}$ **and** λ_s=0)

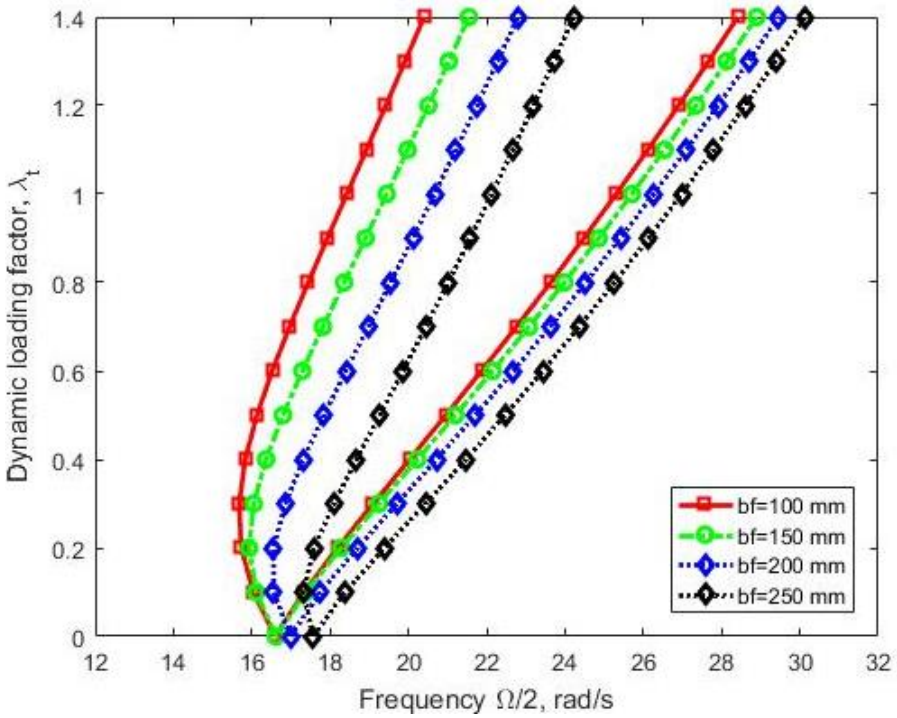

Fig. 9. Comparison of dynamic instability regions of simply supported castellated beams (beam length 14.549 meter) ($\boldsymbol{q_y = q_{cr}}$ **and** $\boldsymbol{\lambda_s}$=0)